Defence Science Journal, Vol. 71, No. 6, November 2021, pp. 807-815, DOI : 10.14429/dsj.71.16791

Perturbation Propagation Models for Underwater Sensor Localisation using Semidefinite Programming

Prateek and Rajeev Arya*

National Institute of Technology Patna, Patna - 800 005, India

**E-mail: rajeev.arya@nitp.ac.in*

ABSTRACT

Real time Underwater sensor networks (UWSNs) suffer from localisation issues due to a dearth of incorporation of different geometric scenarios in UWSN scenarios. To address these issues, this paper visualises three specific scenarios of perturbation. First, small sized and large numbered particles of perturbance moving in a tangential motion to the sensor nodes; second, a single numbered and large-sized particle moving in a rectilinear motion by displacing the sensor nodes into sideward and forward direction, and third, a radially outward propagating perturbance to observe the influenced sensor nodes as the perturbance moves outwards. A novel target localisation and tracking is facilitated by including marine vehicle navigation as a source of perturbation. Using semidefinite programming, the proposed perturbation models minimise localisation errors, thereby enhancing physical security of underwater sensor nodes. By leveraging the spin, cleaving motion and radial cast-away behaviour of underwater sensor nodes, the results confirm that the proposed propagation models can be conveniently applied to real time target detection and estimation of underwater target nodes.

Keywords: Underwater sensor networks localisation; Physical underwater security; Real time underwater sensor surveillance; Perturbation modelling

NOMENCLATURE

a	Anchor nodes
FIM	Fisher Information Matrix
s	Sensor nodes
F_{pr}	Footprint of perturbation
λ	Turbulence
D_λ	Tangential perturbation effect on node turbulence
v	Water density
α_{ij}	Absolute node dispersion
d_i	Displacement of anchor node
P	Number of anchor nodes
β_{ij}	Relative node dispersion
Q	Number of perturbed anchor node pairs
g_i	Anchor node separation
$D(\tau, f)$	Displacement as a function of iteration count and perturbation particles
f	Perturbation particles
$r_v^F(B, A)$	Radial outwards propagation parameter
τ	Iteration count
E_{meas}	Measured error matrix
W	Displacement measurement weight vector
H	Underwater acoustic propagation matrix
z	Observed perturbation
p_{3n}	Perturbation on n^{th} sensor node due to 3^{rd} scenario
μ	Mean of the observations
$iter$	Number of iterations
C	Covariance matrix
$bdiag$	Block diagonal matrix
$diag$	Diagonal matrix
I_{all_nodes}	FIM for target nodes
I_{SPM}	FIM for nodes under SPM
SPM	Spin propagation model
rPM	Radially outwards perturbation model
rDM	Rectilinear dispersion model
sDP	Semidefinite programming
gMM	Gaussian mixture modelling

Received : 05 February 2021, Revised : 05 July 2021
Accepted : 05 August 2021, Online published : 22 October 2021

1. INTRODUCTION

Underwater sensor networks (UWSNs) are a big asset to any Research Organisation simply because humans cannot naturally survive underwater, requiring specialised hardware to explore the depths of the seas and oceans. Since wireless sensor nodes are self-configuring and can suitably operate using acoustic, optical and magnetic propagation underwater, there is keen interest to achieve a robust and accurate UWSN that would survive the harsh environment of deep as well as shallow depth. In literature, a recent survey on the issues faced by UWSNs showed that underwater nodes are susceptible to drift and high delay[1]. As a result, localisation is not able to keep up when anchor nodes do not operate cooperatively[2].

The problem with localisation in UWSNs is that traditional terrestrial methods such as Global Positioning System (GPS) do not work underwater. Therefore, several techniques are being developed to determine accurate location of underwater target, or to position the underwater sensors immaculately. This enables researchers and explorers to monitor underwater environment remotely, for purposes of national as well as international importance such as subsea natural resource exploration, oil rigs maintenance, maritime border surveillance, tsunami and other disaster management, enemy target tracking etc. There is tremendous scope of improvement for a fast, efficient and reliable technique for underwater localisation. The following subsections shall discuss the importance of the problem at hand, and a background of the approaches taken in existing literature.

1.1 Related Work

By taking a variety of scenarios, the localisation performance is dealt with on a one-to-one basis. For example, by increasing the sample sequence length, the error in estimating the shift in doppler spread is minimised quadratically[3]. Doppler shift is combined with genetic algorithm to improve localisation[4]. A probabilistic data approach, which is computationally expensive yet sufficiently accurate, is proposed[5].

1.1.1 Semidefinite Programming

Semidefinite programming (SDP) is popular means of convex formulation[6] to arrive at iterative solution to numerical problems, both constrained as well as unconstrained. It is used for convex optimisation of linear objective functions over the intersection of the cone of positive semidefinite matrices with an affine space. It has been used in terrestrial[7] scenarios to achieve localisation of sensor nodes in WSN. However, to the best of the authors' knowledge, SDP has not been documented in UWSN localisation. Authors in[8] have presented a frame-by-frame cluster configuration to effectively localise the target using acoustic emission. Although they have used sparse sensor array for this purpose and approached acoustic localisation through Doppler shift, however they have not compared their result with semidefinite programming for acoustic spatial localisation.

Use of semidefinite relaxation has enabled[9] to derive localisation for both non-cooperative as well as cooperative case. However, the implementation in this work is limited to radio frequency (RF) based subsystems[10], and does not cater to underwater acoustic systems[11]. The authors[12] have considered classifying moving vehicles as the intended target by using a correlation-based dependence graph and wireless acoustic sensor network. However, the work does not illuminate on the lower bound of the variance for calculating Fisher's Information Matrix, which would be critical to compute Cramer Rao's Lower Bound on the localisation error. Some recent works related to perturbation analysis in underwater sensor networks are mentioned in Table 1.

1.1.2 Underwater Localisation

Wireless Sensor networks capture the essence of parameters in their surroundings. Therefore, the location information associated with every sensed data must be accurate, hence the need for localisation. Underwater localisation enables the user to pinpoint the coordinates of the underwater nodes. Some of the prior works in underwater localisation have been discussed here. Authors[13] have considered three perturbations: asynchronous clock, stratification effect and mobility due to current which affects underwater acoustic sensor network localisation. Using a method of iterative least square estimator, they have been able to compensate for the disturbances and consequently achieve underwater localisation with the assistance of an autonomous underwater vehicle (AUV). However, we know that iterative least square method suffers from estimation errors if the number of samples available are not sufficiently large, for example, in case of sparsely deployed sensor networks. To overcome this issue, the work done by Sun et al.[14] go for the method of 2nd order Time Difference of Arrival (TDOA). They are able to address the issue of drifted signal period under sea where pressure is high and temperature is low. However, multi path environment which is created by heavy clutter, poses a grave issue to underwater localisation. Therefore, the work done by Liu[5], *et al.* attempts to overcome this issue by employing maximum likelihood probabilistic data association with Grid search and PSO to find the optimal target estimate. However, even ML PDA suffers from requirement of a large dataset to work upon. Therefore, a suitable alternate method to achieve commendable performance in terms of underwater localisation would be to derive semidefinite equations subject to appropriate constraints, which is one of the prime contributions of our work.

Table 1. Types of perturbations addressed in recent literature of underwater sensor network localisation.

Localisation algorithm	Type of perturbation addressed	Method used
Yan[13], *et al.*	Motion & ray compensation strategies: Current mobility	Iterative least square estimator
Sun[14], *et al.*	Drifted signal period	2nd Order TDOA
Liu[5], *et al.*	Multipath environment with heavy clutter	Maximum likelihood probabilistic data association with grid search & PSO

1.2 Major Contributions

This paper attempts to contribute to the profession in the following ways:

1. Semidefinite formulation for Underwater sensor networks has been attempted for the first time to achieve localisation. So far most of the existing works have been limited to terrestrial or sensor networks, in general.
2. Convex modelling of vorticity equation in terms of tumble or spin propagation of perturbation is new and has not been attempted so far. The closest work related to this finding[15] does not focus on localisation in aquatic scenario.
3. The paper explores the impact of footprint of perturbance in terms of Cramer Rao Lower Bound (CRLB)[16], which is

a genuine concern in terms of event propagation, on the localisation aspect of UWSN.

In this paper, standard notation for scalar and vector have been used. If A denotes a scalar, then bold representation $\mathbf{A}$ represents a vector. The rest of the paper is organised as follows: a detailed description, followed by mathematical representation of three different perturbation scenarios is discussed in section 2. Section 3 describes the semidefinite formulation of the proposed localisation scenario, followed by derivation of Cramer Rao Lower Bound. Numerical computations and results are discussed in Section 4. Some concluding remarks are mentioned in Section 5.

2. METHODS

Underwater sensor nodes are subject to various adversities. These adversities, or perturbations, as we shall refer to in this paper, may be physically large sized or small sized. The physical dimension influences how the perturbations interact with the anchor nodes. To carry on, let us define the term "footprint" in terms of our paper:

Definition 1: In an underwater sensor network (UWSN), if a denotes anchor nodes and s denotes sensor nodes, then the Footprint of a source of perturbance is represented by F_{pr}, and is given by

$$F_{pr} = \left\{ \# a : \left\| a_{i,t+1} - a_{i,t} \right\|_2 > 0, \forall i \in a, \, t < t_p, \, (t+1) > t_p \right\} \tag{1}$$

If $\#a$ represents the number of nodes affected by the perturbation event, then the time $(t+1)$ is the time after the impact of the perturbation t_p, whereas t is the time before the impact of perturbation. The range of nodes under the influence of perturbation is a broad indication of the footprint of the source of perturbation.

In order to determine the extent of footprint on the localisation performance of the UWSN nodes, it is essential to pinpoint some common types of perturbation propagation styles. In current work, we enumerate three such propagation, and represent their mathematical model which shall be used to localise the anchor nodes subsequently.

2.1 Perturbance Propagation with Trajectory and Footprint Variation

2.1.1 Spin Propagation Model

Due to tangential motion of perturbance along the sensor and anchor nodes, the underwater nodes may physically remain at the same coordinates. However, they may experience a spin or a tumble by certain angle ($0\,rad$ to $2\pi\,rad$) along any plane in the three-dimensional space. This tumbling is akin to yaw, pitch and roll action, and the uncertainty in positioning of the anchor nodes must be mathematically modelled to incorporate spin perturbation. In practical scenarios, tumbling may occur when the source of perturbation has a large number of particles which are physically similar in dimensions to the anchor nodes. The best visualisation is seen when a shoal of fish passes through the sensor network, their perturbation leads to tumbling of sensor nodes underwater. This is illustrated in Fig. 1. The blue objects denote perturbation particles. Brown objects denote underwater sensor nodes, subject to tumble/ spin.

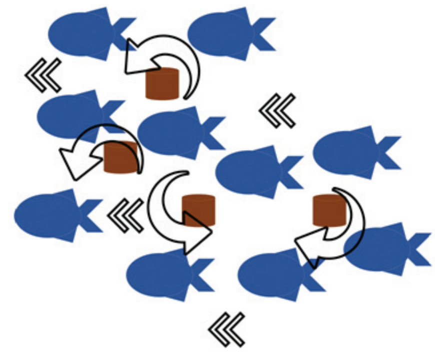

Figure 1. Illustration of spin propagation model.

2.1.2 Rectilinear Model with Angular Spreading

The scenario where inverted v shaped ripples are created, the nodes may get displaced perpendicular to the direction of perturbation propagation. This kind of separation occurs when the physical dimension of perturbation particles is much larger than the nodes themselves, and the motion of perturbation is in a straight-forward fashion. A practical example would be a ship or a submarine or a whale passing through the network of underwater nodes, which would split the water volume into two halves, right and left, as shown in Fig. 2. The brown objects denote perturbation particle, blue curves denote the effect on water, black objects denote underwater sensor nodes, subject to dispersion forward and sideward. The big arrow denotes forward propagation of rectilinear perturbation. Once this scenario is mathematically modelled, the uncertainty associated with the position of anchor nodes may be compensated for, and appropriate localisation techniques shall enhance the updated position of the displaced anchor nodes.

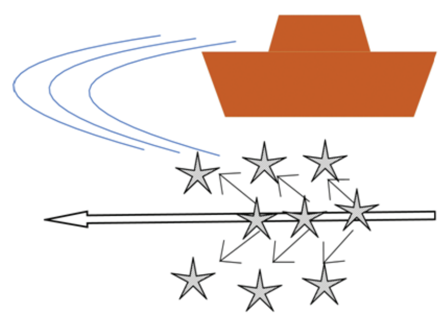

Figure 2. Illustration of rectilinear dispersion model (RDM).

2.1.3 Radially Outwards Propagation Model

In the third scenario, the perturbation propagates in a radially outward manner. The number of nodes affected by this perturbation depends on the radius of perturbation. A sound manner to depict the affected nodes would be to devise an 'engulf factor' to accurately denote the percentage of nodes under the influence of perturbation. A mathematical model should follow the explained scenario. A practical example would be the scene of an oil spill on the surface of the ocean, or the radial outward spreading of crash debris of an aircraft on the surface of water. This is illustrated in Fig. 3. The brown object denotes perturbation source, the blue shapes represent spread of perturbation radially outwards. The small shapes represent underwater nodes subject to engulfment by perturbation.

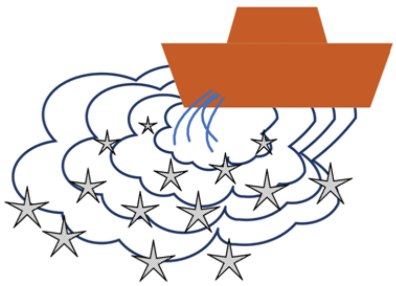

Figure 3. Illustration of radially outward propagation model.

3. MATHEMATICAL FORMULATION

3.1 Semidefinite Programming Formulation

Let us be given a set of Anchor nodes A, a set of sensor nodes S and a set of perturbing particles F in $\mathbb{R}^3$. Due to tangential motion of the perturbance along the sensor nodes and anchor nodes, the nodes may experience a turbulence, causing dislocation from their usual position. Let us denote the turbulence λ faced by the nodes underwater with a constant water density $\nabla \cdot v = 0$. The effect of perturbation tangential motion on the nature of turbulence of the anchor nodes is denoted by D_λ. The rate of change of turbulence of the anchor nodes is defined as the curl of velocity equation

$$\frac{\partial \lambda}{\partial t} + (v \cdot \nabla)\lambda - (\lambda \cdot \nabla)v = D_\lambda \tag{2}$$

Equation is governed by the vorticity transport equation[17]. Then, the cost function to be minimised is given by

$$minimise\left(\frac{\partial \lambda}{\partial t} + (\nu \cdot \nabla)\lambda - (\lambda \cdot \nabla)\nu - D_\lambda\right) \tag{3}$$

Subject to

$$\nabla \cdot \nu = 0 \tag{4}$$

Due to the rectilinear motion of a large single perturbance (such as a ship or a whale or a submarine), the plane containing the sensor nodes and the perturbance, is cleaved into two halves. The distance between previous node position and current node position is quantified by the absolute and relative dispersion. If d_i is the anchor node displacement from its initial position in the x-sideward ($i, j = 1$), and y-forward ($i, j = 2$) and P is the number of anchor nodes, then the absolute dispersion is formulated as

$$\left\langle \alpha_{ij}^2 \right\rangle = \frac{1}{P}\sum_{m=1}^{P} d_i d_j \tag{5}$$

The relative dispersion of the anchor nodes due to cleaving of water into two halves is defined as

$$\left\langle \beta_{ij}^2 \right\rangle = \frac{1}{Q}\sum_{n=1}^{Q} g_i g_j \tag{6}$$

where, g is the sideward ($i, j = 1$) and forward ($i, j = 2$) separations of the anchor node positions, and Q is the number of anchor node pairs affected by the perturbance.

In case of radial perturbation of particles, the distance of displacement of anchor nodes shall be governed by equation mentioned at the bottom of the page for clarity.

where, $f \in F$. f denotes each particle of the set F. F is the set of all perturbance elements which propagate in a radially outward manner and τ is the iteration count for every node displaced by the particle set F. The radial outwards propagation is then modelled as in equation

$$r_v^F(B, A) = \left\{ \begin{matrix} w \cdot D(\tau, f) \mid \forall f \in F, \\ \tau \in [1, \tau_{\max}], \ w \in rand(1,1) \end{matrix} \right\} \tag{7}$$

where, r is the radius of outward propagation of perturbation particle and w is the weight coefficient associated with every displacement D.

The relaxed Semidefinite formulation for Maximum Likelihood estimation of the displaced anchor nodes is given by

$$\min imise\left(Tr\left(W.E_{meas}\right)\right) \tag{8}$$

Subject to

$$W = \begin{bmatrix} H^T.H & -H^T.D_{meas} \\ -D_{meas}^T.H & D_{meas}^T.D_{meas} \end{bmatrix} \succeq 0 \tag{9}$$

$$diag\left(D_{meas}\right) == 1 \tag{10}$$

$$D_{meas} \succeq 0 \tag{11}$$

where, W is the weight vector associated with every displacement measurement D_{meas}, H is the underwater acoustic propagation matrix. The objective function of equation represents the weighted error in measurement of displacement of anchor node. This error is formulated as

$$E_{i,j} = \left\| D_{meas}^{t,t+1} - D_{actual}^{t,t+1} \right\| \tag{12}$$

E is a symmetric matrix with dimensions $n \times n$ where $n = \#a$, that is, the number of affected anchor nodes.

$$D(\tau, f) = \frac{\left(f^2 + 2f + 1\right)2^\tau + 2f + 3}{(2f + 3)} \cdot (f + 2)^{2\tau - 1} +$$

$$(f + 2)^\tau - \frac{(f + 2)^2}{2f + 3} \cdot (f + 2)^{\tau - 1} \tag{13}$$

Cramer Rao Lower Bound (CRLB)

The combined perturbations of three scenarios is to be estimated. Let $z = [p_{11} \ p_{12} \ \cdots \ p_{1n} \ p_{21} \ p_{22} \ \cdots \ p_{2n} \ p_{31} \ p_{32} \ \cdots \ p_{3n}]$ be the observed perturbation due to three scenarios on each of the sensor nodes. For example, p_{12} is the perturbation on the second sensor node due to the scenario of the first kind. Since three scenarios exist, p_{12}, p_{22} and p_{12} denote respectively the effect of first, second and third scenario on sensor node 2. Since perturbance of unaffected nodes is zero, such p_{ij} elements are zero in the z vector. Since observed/ measured vector is corrupted by additive white Gaussian noise, z is also Gaussian distributed with mean μ and covariance matrix C, that is, $z \sim N(\mu, C)$, as shown in equation mentioned at the bottom of this page for clarity.

The covariance matrix C consists of

$$C = bdiag\left(C_{11}, C_{22}, C_{33}\right) \tag{14}$$

where,

$$C_{11} = diag\left(\sigma_{11}^2, \sigma_{12}^2, \cdots, \sigma_{1N}^2\right) \tag{15}$$

$$C_{22} = diag\left(\sigma_{21}^2, \sigma_{22}^2, \cdots, \sigma_{2N}^2\right) \tag{16}$$

$$C_{33} = diag\left(\sigma_{31}^2, \sigma_{32}^2, \cdots, \sigma_{3N}^2\right) \tag{17}$$

and $bdiag$ represents block diagonal matrix, whereas $diag$ represents diagonal matrix. The Fisher Information Matrix (FIM) for target nodes, that is, (x_i, y_i) for sensor nodes and $\left(a_x^i, a_y^i\right)$ for anchor nodes is given as

$$I_{all\_nodes} = HC^{-1}H^T \tag{18}$$

where, H is given by equation ,

or,

$$H = \begin{bmatrix} H_{11} & H_{12} \\ h_{21} & 0 \end{bmatrix}, \tag{19}$$

H_{11} is given by equation ,

$$H_{12} = \begin{bmatrix} I_{2M} & 0_{2M\times(2M-2)} \end{bmatrix}^T \tag{20}$$

$$h_{21} = \begin{bmatrix} r_{1,2} & r_{1,3} & \cdots & r_{(M-1),M} \end{bmatrix} \tag{21}$$

Taking inverse of FIM gives us Cramer Rao Lower Bound CRLB for the lower bound on estimation error of location due to perturbation. When there is only one perturbation, our observation vector remains the same as before, but now two of the three classes of perturbations are known. The corresponding FIM for $\begin{bmatrix} p_{11} & p_{12} & \cdots & p_{1n} \end{bmatrix}^T$, denoted by I_{SPM}, is modified as

$$I_{SPM} = H_{11}C_{11}^{-1}H_{11}^T + H_{12}C_{22}^{-1}H_{12}^T \tag{22}$$

4. LOCALISATION PERFORMANCE AND DISCUSSION

Simulations has been carried out using semidefinite program solver CVX in MATLAB. The default solver SDPT3 has been used. Computations have been run for different node densities, (anchor nodes and sensor nodes). The anchor node positions are fixed at corners and symmetric locations while the sensor node positions are randomly deployed. Anchor node counts are varied in the range of 5 to 16. Non anchor node count is set to 15 and 30, respectively. Different transmission power of the anchor and sensor nodes is represented by setting different signal to noise ratio per scenario. Anchor perturbation is varied between 0 and 2, whereas noise variance is set to 2 to 7. Low perturbation scenario is simulated by keeping 3 to 7 number of perturbation objects, whereas moderate perturbation scenario is simulated with the help of 9 to 10 perturbation objects. A fixed area of $100\times100\,m^2$ has been used to deploy these nodes, as summarised in Table 2.

Table 2. Localisation parameters

Parameter	Symbol	Range
Dimension of sensor deployment area		$100\times100m^2$
Anchor node count		5 to 16
Non- anchor node count		15,30
Standard deviation of anchor perturbation	σ_α	0 to 2
Transmitted SNR (dB)		20, 30, 40, 50
Noise variance		2 to 7
Number of Perturbation objects		3, 5, 7, 9, 10

A broad representation of the geometric arrangement of deployed nodes is shown in Fig. 4. Anchor nodes are denoted by large circles whereas sensor nodes are shown as small squares. Fig. 4(a). is a regular 3 by 3 arrangement of anchor nodes. Pentagonal anchor node geometry is shown in Fig. 4(b). Hexagonal geometry follows next, in part (c), and octagonal geometry in (d).

$$\mu = \begin{bmatrix} \frac{\sum_{i=1}^{iter} D_{\lambda,1,1,i}}{iter} & \frac{\sum_{i=1}^{iter} D_{\lambda,1,2,i}}{iter} & \cdots & \frac{\sum_{i=1}^{iter} D_{\lambda,1,N,i}}{iter} & \frac{\sum_{i=1}^{iter} \alpha_{2,1,i}}{iter} & \frac{\sum_{i=1}^{iter} \alpha_{2,2,i}}{iter} & \cdots & \frac{\sum_{i=1}^{iter} \alpha_{2,N,i}}{iter} & \frac{\sum_{i=1}^{iter} r_{1,1,i}}{iter} & \frac{\sum_{i=1}^{iter} r_{1,2,i}}{iter} & \cdots & \frac{\sum_{i=1}^{iter} r_{1,N,i}}{iter} \end{bmatrix}^T \tag{23}$$

$$H = \begin{bmatrix} \frac{\partial\mu}{\partial s_x^1} & \frac{\partial\mu}{\partial s_y^1} & \frac{\partial\mu}{\partial s_x^2} & \frac{\partial\mu}{\partial s_y^2} & \cdots & \frac{\partial\mu}{\partial s_x^M} & \frac{\partial\mu}{\partial s_y^M} & \frac{\partial\mu}{\partial a_x^1} & \frac{\partial\mu}{\partial a_y^1} & \frac{\partial\mu}{\partial a_x^2} & \frac{\partial\mu}{\partial a_y^2} & \cdots & \frac{\partial\mu}{\partial a_x^M} & \frac{\partial\mu}{\partial a_y^M} \end{bmatrix}^T \tag{24}$$

$$H_{11} = \begin{bmatrix} \frac{(p_{1,1}-p_{2,1})}{r_{1,2}} & \frac{(p_{1,1}-p_{3,1})}{r_{1,3}} & \cdots & \frac{(p_{1,1}-p_{M,1})}{r_{1,M}} & 0 & 0 & \cdots & 0 \\ 0 & 0 & \cdots & 0 & \frac{(p_{1,2}-p_{2,1})}{r_{2,1}} & \frac{(p_{1,2}-p_{3,1})}{r_{2,2}} & \cdots & 0 \\ \vdots & \vdots & \ddots & \vdots & \vdots & \vdots & \ddots & \vdots \\ 0 & 0 & \cdots & \frac{(p_{M,1}-p_{1,1})}{r_{1,M}} & 0 & 0 & 0 & \frac{(p_{M,1}-p_{M-1,1})}{r_{M,M-1}} \end{bmatrix} \tag{25}$$

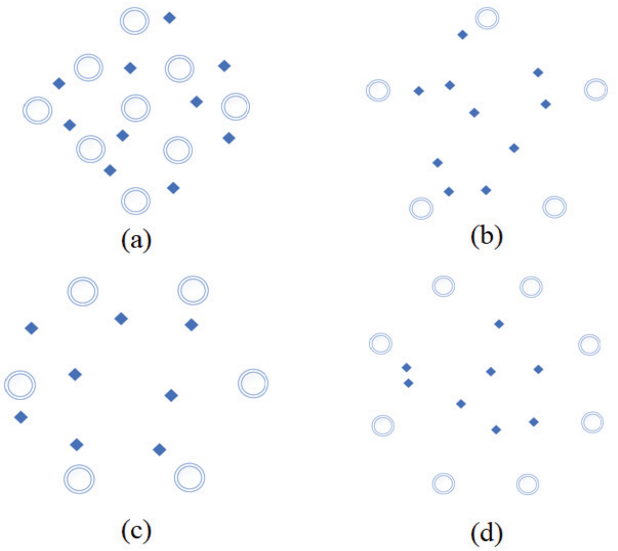

Figure 4. Vacuolation of node geometric arrangements used in evaluation of the proposed localisation. (a) rectangular, (b) pentagonal, (c) hexagonal, and (d) octagonal anchor node arrangement.

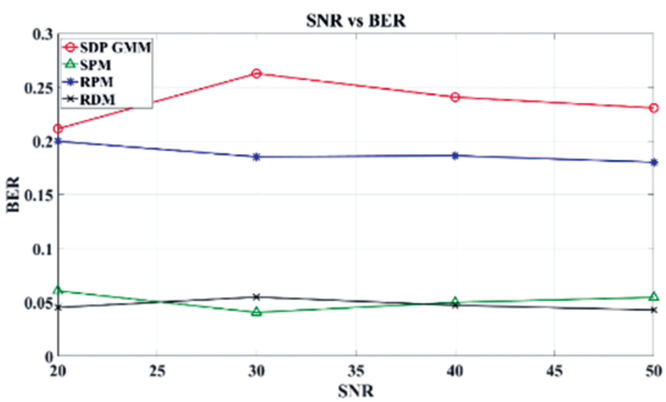

Figure 5. BER to SNR performance of different perturbation models.

Results of Spin Propagation Model (denoted by SPM in figures), Radially outwards Perturbation Model (RPM), Rectilinear Dispersion Model (RDM) are compared to a Gaussian Mixture Model[18] based on Semidefinite programming model (denoted by SDP GMM). The Bit error rate vs. signal to noise ratio of different localisation models are depicted in Fig. 5. The best performance in terms of minimum BER is achieved by RDM at the cost of high transmission power. A closely trailing performance is observed by SPM, owing to its nature of getting displaced only in terms of orientation but negligibly displaced in terms of physical coordinates, especially for intermediate signal strength. The radial propagation model fared up to four times higher bit error rates than RDM or SPM, nearing the performance of Gaussian mixture model for most of the cases.

In terms of RMS errors, the localisation performance comparison is shown in Fig. 6. for different numbers of anchor nodes. Here, SPM performs the best when a total of 8 anchor nodes are deployed. The linear Dispersion model fares the best at the cost of requiring the maximum number

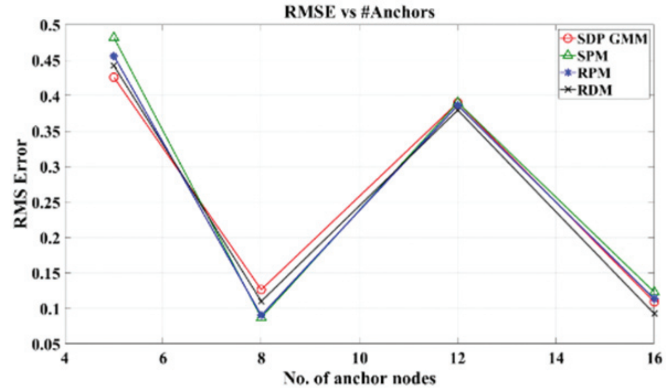

Figure 6. Localisation error performance of different perturbation models.

of anchor nodes, and hence the higher SNR requirement. The semidefinite programming method based on Gaussian Mixture Model is also shown for comparison. The dip in RMS error for 8 and 16 number of anchor nodes is because such anchor nodes have lower node uncertainty than the rest, leading to a more efficient triangulation of target. For further insights, one may go through the concept of triangulation uncertainty for optimal node positioning[23]. Localisation error performance is dependent highly on the node geometry. Since anchor nodes geometry has been kept symmetric, hence the closeness of all the methods To distinguish further, Fig. 7(a) is important because it describes error performance with respect to noise

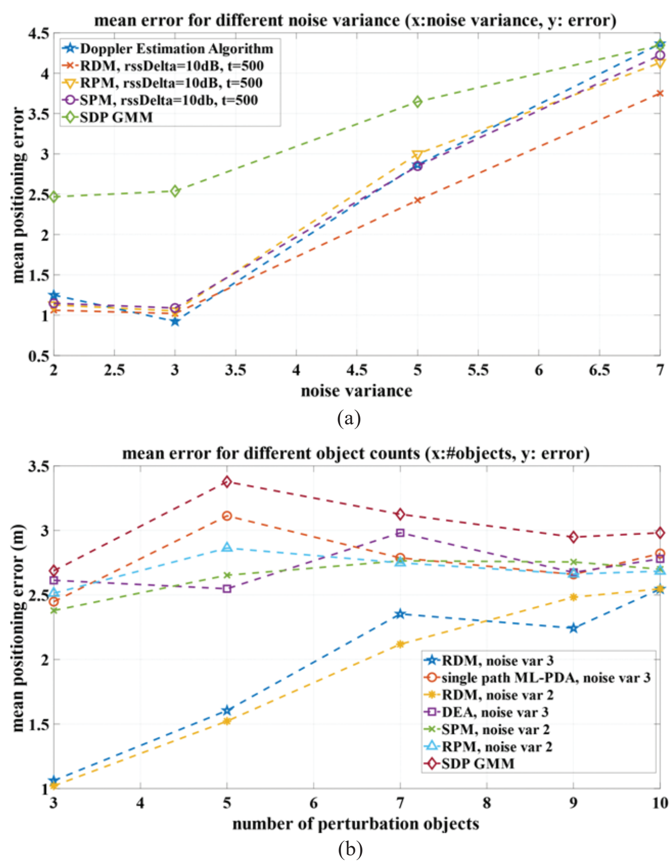

Figure 7. (a) Effect of noise variance on the localisation of target in presence of perturbations and (b) Dependence of various localisation algorithms on the number of perturbation objects.

variance. The disparities may be observed more clearly. Moreover, for a given perturbing agent, the three types of perturbations, namely radial, rectilinear and Spin have partial contribution to the overall perturbation in water. This can be concurred since motion in water rarely comprises of single perturbation alone, and usually it is a linear combination all the three. That is why further RMS error performance has been demonstrated in Fig. 7(b) to distinguish performance of various methods with respect to perturbation count also."

Further analysis of the proposed technique may be carried out using noise variance and number of perturbation objects as the key parameters. For the case of different noise variance, the transmissions from the target node are assumed to attenuate a maximum of 10dB before declaring localisation failure. For uniformity, the perturbation is allowed to disturb the surrounding node deployments for a duration of 500 seconds. Anchor nodes get displaced or tumbled from their initial states due to the perturbations and instantaneously transmit beacon signals in order to update their new position. The return transmission regarding the new position is exchanged with the nearby sensor nodes. Based on the constraints offered by the respective semidefinite formulations, the sensor nodes attempt to nullify the error between current location and the predicted location. A lower positioning error closer to zero indicates a higher localisation accuracy. Under high perturbation loads the rectilinear dispersion model (RDM) is observed to perform better than the competing models. From the noise variance plots of Fig. 7(a), it is evident that RDM locates the user more accurately at larger noise variances while being comparable to the RPM & SPM methods proposed in this paper at smaller noise variances. It has been clear that the various kinds of perturbation sizes and counts have a profound effect on the type of localisation on offer. Although the Doppler Estimation Algorithm discussed in[3] is computationally simple and tries to overcome localisation errors based on calculation of Doppler Shift between the target node and the anchor node, it falls behind the perturbation models when dealing with the issue of three perturbations discussed in the current work. The dip in error for noise variance 3 may be attributed to the compensation of perturbation effects that overcomes positioning disparity, in accordance with sensor node topology[24].

Table 3. Comparison of proposed technique with existing works on underwater localisation

Localisation algorithm	Reference	Characteristic parameter	Improvement

• Second Order TDOA
• Target tracking algorithm based on particle filter
	Sun[20], *et al.*	Analysis of
		• Horizontal dilution of precision (HDOP)
		• Precision of Localisation based on
		  o Depth of AUV
		  o Depth of Black box
		  o Sound Speed
		  o RMSE of arrival direction
		Localisation with
		• Circular path
		• Linear path
		Tracking with
		• Circular path
		• Linear path
			• Elimination of unknown signal period
			• Higher precision than DoA-based methods.

• Multilateration • Hidden Markov model with forward-backward algorithm	Alexandri[21], *et al.*	Analysis of • Resolved ambiguities • Unresolved ambiguities	• Extrapolation of positions in data series for superior tracking • Rigorous localisation of marine animals
Detection, direction of arrival and clustering	Stinko[22], *et al.*	Analysis of • Acoustic pressure • Components of particle velocity vector Estimation of DoA of noise sources	• Detection of low frequency noise sources • Accurate bearing estimates of target due to AUV • Feasibility of acoustic modem and USBL positioning system on a glider
• Two asynchronous localisation algorithms to localise active and passive sensor nodes • Iterative Least squares technique to estimate unknown water current parameters	Yan[13], *et al.*	Incorporation of • motion and ray compensation strategies into localisation • Current field estimation technique	Elimination of • Asynchronous • Stratification clock effect • Node Mobility
Proposed method (SDP formulation for sensor node localisation subject to three major underwater perturbations)		Analysis of • Degradation in localisation accuracy due to three different underwater perturbations	• Superior localisation despite onset of realistic perturbation effects • Effective perturbation compensation with the help of semidefinite programming • Comparable positioning error across various scenarios, similar to Gong *et al.*[3]

Further, the proposed model is compared to the technique of single-path Maximum Likelihood Probabilistic Data Association[19]. For a low perturbation scenario of 3 and 5 objects, respectively, as shown in Fig. 7(b), the single path ML-PDA technique spikes to an error beyond 3m, whereas the SDP-GMM method could handle error around 3.5m, which demonstrates superior localisation ability of the proposed methods. In comparison, the Doppler Estimation Algorithm carries a lower penalty than ML-PDA and SDP-GMM[18] method, while still being inferior to the proposed RDM method.

Looking at Figs. 7(a) and 7(b), it may be observed that under different scenarios, at least one of the three proposed perturbation models (SPM, RDM, RPM) performs suitably to give accurate target localisation results. A comparison of the proposed technique with the existing methods is tabulated in Table 3.

5. CONCLUSION

A novel technique of perturbation footprint for underwater sensor node localisation was proposed using Semidefinite Programming. Using scenarios consisting of three different types of perturbations, mathematical models were constructed to be incorporated into the semidefinite programming model to yield enhanced physical security of the underwater scenario. Smart surveillance and underwater target tracking analysis exhibited the strengths and limitations of the proposed models in this paper. Based on numerical computations, we concluded that the Rectilinear programming model fares appreciably at high node densities. We also concluded that the effect of tumbling of anchor nodes under SPM incurs minimum harm to localisation, whereas the most difficult scenario is when perturbation particles disperse radially outwards because the search space increases exponentially with increase in the radius of spread. To mitigate these issues, the proposed semidefinite model based on perturbation scenario was found to be able to localise underwater nodes effectively in two of the total four anchor node configurations. Moreover, the proposed formulation achieved lower bit error rate in all the three scenarios as compared to existing techniques such as Gaussian Mixture Model. In terms of low noise variance, the proposed methods were equally good or superior, whereas in noise cluttered environment, the rectilinear dispersion model (RDM) exhibited strong localisation accuracy. Extensive analysis was also carried out by considering different counts of perturbation objects. The proposed models are able to demonstrate positioning error comparable to the state-of-the-art techniques especially at different number of perturbation objects.

REFERENCES

1. Awan, K. M.; Shah, P. A.; Iqbal K.; Gillani S.; Ahmad, W. & Nam, Y. Underwater wireless sensor networks: a review of recent issues and challenges. *Wirel. Commun. Mob. Comput.* 2019, **2019**, 1–20. doi: 10.1155/2019/6470359
2. Gong, Z.; Li, C. & Jiang, F. AUV-aided joint localization and time synchronization for underwater acoustic sensor networks. *IEEE Signal Process. Lett.,* 2018, **25**(4), 477–81. doi: 10.1109/LSP.2018.2799699.
3. Gong, Z.; Li, C. & Jiang, F. Analysis of the underwater multi-path reflections on Doppler shift estimation. *IEEE Wirel. Commun. Lett.,* 2020, **9**(10), 1758–62. doi: 10.1109/LWC.2020.3003743
4. Datta, A. & Dasgupta, M. On accurate localization of sensor nodes in underwater sensor networks: a Doppler shift and modified genetic algorithm based localization technique. *Evol. Intell.,* 2020. doi: 10.1007/s12065-019-00343-1
5. Liu, B.; Tang, X.; Tharmarasa, R.; Kirubarajan, T.; Jassemi, R. & Halle, S. Underwater target tracking in uncertain multipath ocean environments. *IEEE Trans. Aerosp. Electron. Syst.,* 2020, **56**(6), 4899–915. doi: 10.1109/TAES.2020.3003703
6. Zheng, Y.; & Yamane, K. Generalized Distance Between Compact Convex Sets: Algorithms and Applications. *IEEE Trans. Robot.,* 2015, **31**(4), 988–1003. doi: 10.1109/TRO.2015.2451411
7. Zou, Y.; & Liu, H. TDOA localization with unknown signal propagation speed and sensor position errors. *IEEE Commun. Lett.,* 2020, **24**(5), 1024–7. doi: 10.1109/LCOMM.2020.2968434
8. Drioli, C.; Giordano, G.; Salvati, D.; Blanchini, F. & Foresti, G. L. Acoustic Target Tracking Through a Cluster of Mobile Agents. *IEEE Trans. Cybern.,* 2019, 1–14. doi: 10.1109/tcyb.2019.2908697
9. Wang, Z.; Zhang, H.; Lu, T. & Gulliver, T. A. Cooperative RSS-based localization in wireless sensor networks using relative error estimation and semidefinite programming. *IEEE Trans. Veh. Technol.,* 2019, **68**(1), 483–97. doi: 10.1109/TVT.2018.2880991
10. Kumar, B.; Sharma, P. & Singh, D. Development of scale and rotation invariant neural network based technique for detection of dielectric contrast concealed targets with millimeter wave system. *Def. Sci. J.,* 2017, **67**(6), 674. doi: 10.14429/dsj.67.11452
11. Saini, T. K. & Sharma, S. C. Context aware routing to assist routing decisions for quality improvement in multi hop ad hoc networks. *Def. Sci. J.,* 2021, **71**(1), 46–54. doi: 10.14429/dsj.71.16067
12. Ntalampiras, S. Moving vehicle classification using wireless acoustic sensor networks. *IEEE Trans. Emerg. Top. Comput. Intell.,* 2018, **2**(2), 129–38. doi: 10.1109/TETCI.2017.2783340
13. Yan, J.; Guo, D.; Luo, X. & Guan, X. AUV-aided localization for underwater acoustic sensor networks with current field estimation. *IEEE Trans. Veh. Technol.,* 2020, **69**(8), 8855–70. doi: 10.1109/TVT.2020.2996513
14. Sun, S.; Zhao, C.; Zheng, C.; Zhao, C. & Wang, Y. High-precision underwater acoustical localization of the black box based on an improved TDOA algorithm. *IEEE Geosci. Remote Sens. Lett.,* 2020, 1–5. doi: 10.1109/LGRS.2020.3002169
15. Ramírez-Mendoza, R.; Murdoch, L.; Jordan, L. B.; Amoudry, L.O.; McLelland, S. & Cooke, R.D. Asymmetric effects of a modelled tidal turbine on the flow and seabed.

Renew. Energy, 2020, **159**, 238–49.
doi: 10.1016/j.renene.2020.05.133

16. Lui, K. W. K.; Ma, W. K.; So, H. C. & Chan, F. K. W. Semi-definite programming algorithms for sensor network node localization with uncertainties in anchor positions and/or propagation speed. *IEEE Trans. Signal. Process.,* 2009, **57**(2), 752–63.
doi: 10.1109/TSP.2008.2007916
17. Vybulkova, L.; Vezza, M. & Brown, R. Simulating the wake downstream of a horizontal axis tidal turbine using a modified vorticity transport model. *IEEE J. Ocean. Eng.,* 2016, **41**(2), 296–301.
doi: 10.1109/JOE.2015.2429231
18. Zhang, Y.; Xing, S.; Zhu, Y.; Yan, F. & Shen, L. RSS-based localization in WSNs using Gaussian mixture model via semidefinite relaxation. *IEEE Commun. Lett.,* 2017, **21**(6), 1329–32.
doi: 10.1109/LCOMM.2017.2666157
19. Cheng, L.; Li, Y.; Xue, M. & Wang, Y. An indoor localization algorithm based on modified joint probabilistic data association for wireless sensor network. *IEEE Trans. Ind. Informatics,* 2021, **17**(1), 63-72.
doi: 10.1109/TII.2020.2979690
20. Sun, S.; Zhang, X.; Zheng, C.; Fu, J. & Zhao, C. Underwater acoustical localization of the black box utilizing single autonomous underwater vehicle based on the second-order time difference of arrival. *IEEE J. Ocean. Eng.,* 2020, **45**(4), 1268–79.
doi: 10.1109/JOE.2019.2950954
21. Alexandri, T.; Shamir, Z. Z.; Bigal, E.; Scheinin, A.; Tchernov, D. & Diamant, R. Localization of acoustically tagged marine animals in under-ranked conditions. *IEEE Trans. Mob. Comput.,* 2021, **20**(3), 1126–37.
doi: 10.1109/TMC.2019.2959765
22. Stinco, P.; Tesei, A.; Ferri, G.; Biagini, S.; Micheli, M. & Garau, B. Passive Acoustic Signal Processing at Low Frequency With a 3-D acoustic vector sensor hosted on a buoyancy glider. *IEEE J. Ocean. Eng.,* 2021, **46**(1), 283–93.
doi: 10.1109/JOE.2020.2968806
23. Prateek & Arya, R. C-TOL: Convex triangulation for optimal node localization with weighted uncertainties. *Phys. Commun.*, 2021, **46**, 101300.
doi: 10.1016/j.phycom.2021.101300
24. Prateek; Arya, R. & Verma, A. K. Non-coherent localization with geometric topology of wireless sensor network under target and anchor node perturbations. *Wirel. Networks*, 2021, **5**(3), 2271-2286.
doi: 10.1007/s11276-021-02575-5

CONTRIBUTORS

Mr Prateek received his BTech in ECE from SPSU Udaipur India in 2014 and MTech in Communication System Engineering from KIIT Bhubaneswar, India in 2017. He is currently pursuing PhD in the Department of Electronics and Communication Engineering at National Institute of Technology Patna, Bihar India. His research interests include Wireless Communication and Soft Computing Techniques.
Contribution in the current study, he did conceptualisation, simulation and computation as well as analysis of result.

Dr Rajeev Arya received PhD in Communication Engineering from Indian Institute of Technology (IIT Roorkee), Roorkee, India in 2016. He has received Ministry of Human Resource Development Scholarship (MHRD India) during M.Tech and PhD. He is currently working as an Assistant Professor with the Department of Electronics & Communication Engineering at National Institute of Technology, Patna, India. His current research interests are Communication Systems & Wireless Communication.
Contribution in the current study, he did problem formulation, and supervise the overall research.